

Thermal Performances of Hybrid Pin Fin with Connector Heat Sink Under Natural Convection

Rosnadiyah Bahsan^{1*}, Muhammad Aniq Asyraf Mohd Zamri¹, Alhassan Salami Tijani¹, Jeeventh Kubenthiran¹, Sajith Thottathil Abdulrahman² and Ibrahim Kolawole Muritala³

¹*School of Mechanical Engineering, College of Engineering, Universiti Teknologi MARA, 40450 UiTM, Shah Alam, Selangor, Malaysia*

²*Department of Mechanical Engineering, KMEA Engineering College, Kuzhivelippady, Edathala P.O., Cochin, Kerala, India*

³*Institute of Low-Carbon Industrial Processes, Department of Low Carbon Reducing Agents, Deutsches Zentrum für Luft- und Raumfahrt (DLR) / German Aerospace Centre, HSZG-Campus Haus Z VII, Schwenninger Weg 1, 02763 Zittau, Germany*

ABSTRACT

Heat transfer in engineering applications has shown progress, especially in electronic devices that raise the need for better heat sink designs. In addition, the generation of heat in devices and electronic circuits has also augmented, leading to the problem of heat dissipation. This study investigates the thermal and fluid flow characteristics of different geometrical configurations of pin fin heat sink under natural convection. The heat sink models studied are Hybrid Pin Fin with Connector Heat Sink (HPFWC HS) and Pin Fin with Connector Heat Sink (PFWC HS). All heat sinks models were simulated using CFD Ansys to analyse each heat sink's thermal performances and flow fields. The results show that adding wings to the HPFWC HS significantly increased heat dissipation. In terms of heat transfer characteristics, the HPFWC HS has about a 5.78% increase in Nusselt number compared with PFWC HS. The reason is that the heat sink HPFWC HS has wings around

it, and these wings help to promote vortex formation around the fins, which leads to a higher heat transfer coefficient. A fin spacing of 15mm is the best spacing for the heat sink compared to other fin spacing.

ARTICLE INFO

Article history:

Received: 18 June 2021

Accepted: 15 December 2021

Published: 25 May 2022

DOI: <https://doi.org/10.47836/pjst.30.3.18>

E-mail addresses:

aniqqasyraf@gmail.com (Muhammad Aniq Asyraf Mohd Zamri)

rosnadiyah@uitm.edu.my (Rosnadiyah Bahsan)

alhassan@uitm.edu.my (Alhassan Salami Tijani)

sar.me@kmeacollege.ac.in (Sajith Thottathil Abdulrahman)

jeeventh@hotmail.com (Jeeventh Kubenthiran)

ibrahim.muritala@dlr.de (Ibrahim Kolawole Muritala)

* Corresponding author

Keywords: Connector heat sink, electronic devices, fin spacing, heat transfer, hybrid fin pin, natural convection

INTRODUCTION

The development of machines and the widespread use of electronic devices have kept growing since the industrial era. The growth and evolution of the industrial revolution evolved exponentially to fulfil the needs and demands of the global industry (Immerman, 2017). Almost all machines are now focusing on automation, including the evolution of small electronic devices. Recent advances in electronic devices such as inverters, computers, transformers, and mobile phones have led to inadequate heat dissipation in these devices; hence the life span is reduced. During the operation of these electronic devices, heat is generated and must be dissipated as much as possible to avoid any malfunction of the systems (Schelling et al., 2005). Failure to dissipate the heat from the components and devices can affect their reliability and performance (Humphries, 2014).

Conduction and convection heat transfers are the most widely used heat transfer or heat dissipation through a medium in thermal management. Convection can be classified into two parts, namely, forced and natural convection. Forced convection, also known as active cooling, is the forced flow of fluid over a solid surface, while natural convection is also known as passive cooling; it depends on the difference in fluid buoyancy effect for heat dissipation from a solid surface (Vijay, 2019). Although forced convection is more efficient to transfer heat than natural convection, it is less reliable due to external devices such as fans or pumps (Joo & Kim, 2015). In addition, devices with frictional components have less reliability because these components deteriorate over time. Therefore, it gives an advantage to natural convection that has high reliability (Meng et al., 2018). Nada and Said (2019) studied the effects of fins geometries, arrangements, dimensions and number of fins on heat transfer due to natural convection and found that as the number of the fins increases, the effective thermal conductivity also increases.

The heat sink is a device used to remove or dissipate unwanted heat from electronic components to the surroundings. Heat sinks can keep the temperature of electronic devices at an optimum level and are used in many applications such as electronic devices, refrigeration, and heat engines (Kumar et al., 2016). Several heat sinks have different geometry, material, or even thermal characteristics. For example, fins are usually used in electronic devices and engineering applications to enhance the convective heat transfer with a large total surface area in a limited space (Jassem, 2013).

A considerable amount of literature has been published on investigating different geometrical configurations of the heat sink. Arefin (2016) stated that a pin fin heat sink with one-degree expansion performs better than the conventional zero-degree expansion in terms of heat transfer. At the same time, Haghighi et al. (2018) studied both plate and pin fin heat sinks and found out that increasing the number of fins causes better heat transfer, but the pressure drop penalty increases; there is, therefore, the need for optimisation of the geometrical configuration of the heat sink. Some authors also add perforations to the heat

sink to increase the heat sink's convective heat transfer rate (Zaidshah & Yadav, 2019). Ibrahim et al. (2018) stated that the heat transfer coefficient for a fin with perforations is higher compared to a non-perforated fin. The best perforation shape, better than any other shape, is a triangular perforated shape. Adding some features to the pin fin or plate fin could increase the heat transfer rate of a heat sink. Choudhary et al. (2019) have studied the presence of wings on pin fin and found that pin fin with wings has better heat transfer results with a moderate rise in frictional losses, and increasing the wings size resulted in a decrease in Nusselt number with increment in frictional losses.

This research investigates the thermal performances of a new design heat sink: Hybrid Pin Fin with Connector Heat Sink (HPFWC HS) and Pin Fin with Connector Heat Sink (PFWC HS). All heat sinks models were simulated using CFD Ansys to observe each heat sink's thermal performances and flow fields. Furthermore, thermal characteristics of the heat sinks such as Nusselt number, Rayleigh number, Prandtl number and heat transfer coefficient were also investigated.

METHODOLOGY

Hybrid Pin Fin with Connector Heat Sink

Two heat sinks have been investigated: Hybrid Pin Fin with Connector Heat Sink (HPFWC HS) and Pin Fin with Connector Heat Sink (PFWC HS). The Hybrid Pin Fin indicates the hybridisation of the conventional pin fin with structured plate fins or wings around the pin fins. Figures 1 and 2 show the HPFWC HS dimensions and PFWC HS, respectively.

The arrangement of pin fins on both heat sinks was in staggered form. The cross-sectional area of the base of the PFWC HS is $75\text{mm} \times 75\text{mm}$, the thickness of 5mm and the diameter pin fin is 6mm . The HPFWC HS also has a base plate area of $75\text{mm} \times 75\text{mm}$ and a thickness of 5mm . The length of the connector depends on the fin spacing. Higher fin spacing means higher connector length. For example, the length of the connector for 15mm fin spacing is approximately 9mm . Table 1 shows the detailed specifications of both

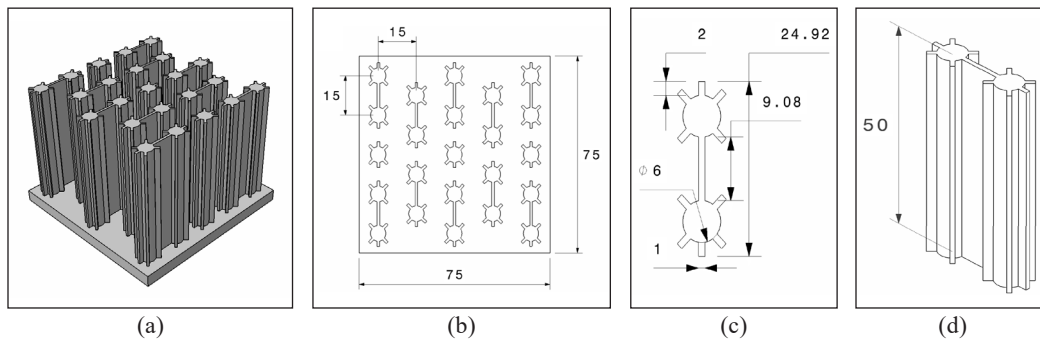


Figure 1. (a) Isometric view of HPFWC HS (b) Top view of HPFWC (c) Top view and dimensions of HPFWC (d) Isometric view and height of HPFWC

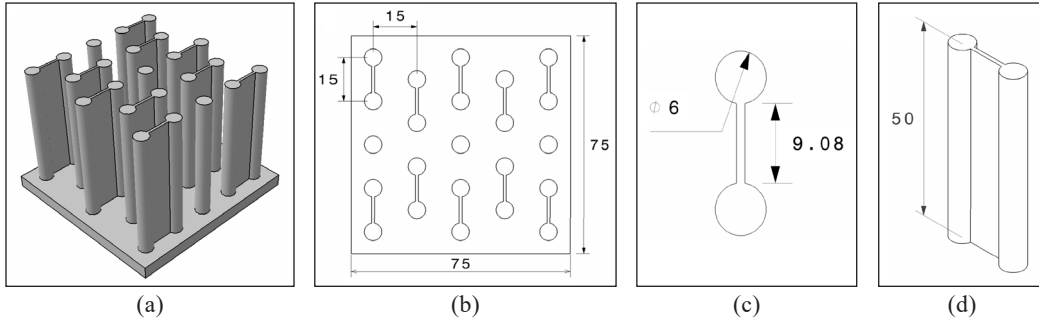


Figure 2. (a) Isometric view of PFWC HS (b) Top view and dimension of PFWC (c) Top view and dimension of PFWC (d) Isometric view and height of PFWC

heat sinks with different configurations. In this study, each design configuration was further modified into Type 1, Type 2 and Type 3. Details of the different types of geometries can be found in Table 1.

Table 1
Heat sinks configurations

Heat sink	H (mm)	W (mm)	S (mm)	D (mm)	N_{pf}	N_c
PFWC Type 1	50	-	15	6	23	10
PFWC Type 2	50	-	20	6	11	6
PFWC Type 3	50	-	25	6	7	2
HPFWC Type 1	50	10	15	6	23	10
HPFWC Type 2	50	10	20	6	11	6
HPFWC Type 3	50	10	25	6	7	2

Aluminium was selected as the material for the heat sink due to its high thermal conductivity (Zagala, 2016) and cost-effectiveness in most applications (Perry, 2017).

Modelling and Simulation

The geometric modelling of the design of all heat sinks is done by using CATIA V5R20 software. Then, the models are imported into Ansys 16 software to undergo Computational Fluid Dynamics (CFD) simulation under Fluent. CFD simulation's main purpose is to numerically determine the fluid behaviours around the heat sinks and investigate the thermal performances of heat sinks under natural convection.

Figure 3 shows the heat sink inside the fluid domain. The size of the domain that was used is $(200 \times 200 \times 300)$ mm (Effendi et al., 2018). The boundary conditions are set on the domain and the heat sink. The domain has one inlet, one outlet, one heated area, and other surfaces set as walls. A mesh model for the heat sinks was created to reduce the degree of freedom from infinite to finite (Jensen, 2018). Figure 4 shows the meshing models of both HPFWC HS and PFWC HS, respectively.

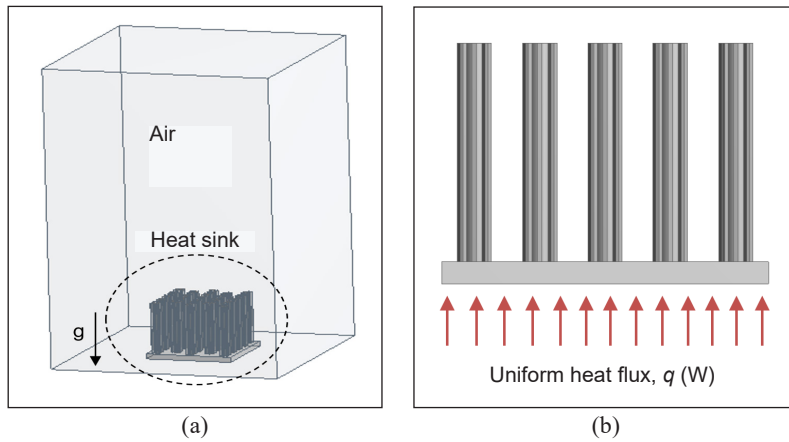


Figure 3. (a) Heat sink in the domain (b) Zoomed heat sink with uniform heat flux

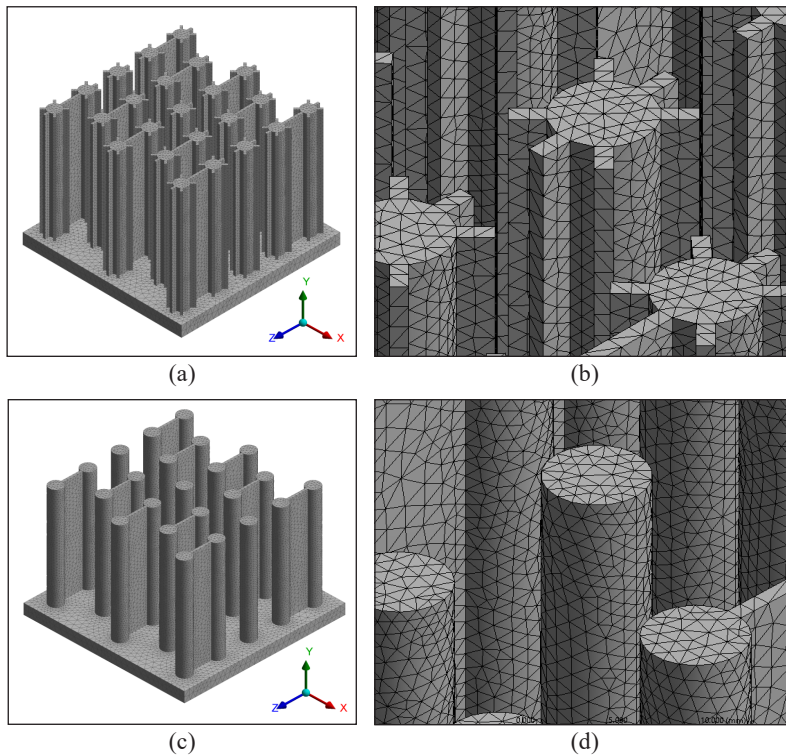


Figure 4. Meshing model of (a) HPFWC HS, (b) the zoomed part of HPFWC, (c) PFWC HS and (d) the zoomed part of PFWC

The fluid used for the heat exchange medium is steady and incompressible air. The ambient temperature is 25°C with inlet and outlet pressure at 1 atm. The base of the heat sink is heated from 5W to 30W. Meshing elements are around 1–2M for all designs with tetrahedra-type elements. The pressure-based solver type and SIMPLE pressure-velocity

coupling, and constant density model were set in the solution models. The pressure discretisation was done based on weighted body force, and gradient discretisation was based on the least square cell-based. In contrast, momentum and energy equations discretisation were carried out based on second-order upwind. Table 2 shows the numerical and boundary conditions used during the calculation (Effendi et al., 2018).

Convergence of numerical equations. The average relative error was computed for every iterative step using Equation 1.

$$R_c = \frac{1}{n.m} \sum_{i=1}^m \sum_{j=1}^n \left| \frac{(F_{i,j}^{S+1} - F_{i,j}^S)}{F_{i,j}^{S+1}} \right| \quad [1]$$

Where F = Unknown parameter such as Temperature (T)
 s = number of iterations
 (i,j)= the grid coordinate

It ensures a convergence solution for the operating variables such as temperature. The solution of the integrated model equations is terminated whenever the relative error between two subsequent solutions is equal to the convergent criteria. In the present study, convergence criteria are attained if Rc is below 10^{-5} for both Continuity equations and temperature, and convergence criteria are reached if Rc is below 10^{-5} for the energy equation.

Grid Independence Test

A grid independence test is carried out to determine the most suitable number and size of the elements to carry out the simulation. During the meshing process, the size of each element was varied and adjusted to increase the accuracy of the simulation. Smaller elemental size means an increment in the number of elements. A higher number of elements tend to result in high accuracy, but the simulation running time is dragged. The grid size and computational domain were carefully chosen such that there is a minimal variation of the physical parameter of interest, such as temperature. Table 3 summarises all elemental sizes, ranging from 18mm to 6mm. The test was carried out on PFWC HS Type 1 with a heat

Table 2
 Summary of numerical and boundary conditions

<i>Physical conditions</i>	
Fluid	Steady and incompressible air
Fluid volume (L × W × H)	200 × 200 × 300 (mm)
Heat sink material	Aluminium
<i>Boundary and thermal conditions</i>	
Air temperature	25°C
Ambient pressure	1 atm
Heat flux	888.89~5333.33 W/m ²
<i>Computational elements</i>	
Number of elements	1-2M elements
Elements type	Tetra
<i>Solution models</i>	
Viscous model	Laminar
Solver type	Pressure based
Pressure-velocity coupling	SIMPLE
Density model	Constant
<i>Spatial discretisation</i>	
Pressure	Body force weighted
Momentum	Second-order upwind
Gradient	Least square cell-based
Energy	Second-order upwind

flux of 5W. Five different element sizes were tested. Table 3 shows that the temperature started to be constant at an element size of 9mm at the number of elements of 1377670. The element size of 6mm gives the highest number of elements, 2514225. The difference in temperature between these two sizes of elements is the lowest compared to other sizes. Since the difference is not very significant, the element size chosen to run the calculations is 9mm.

Table 3
Summary of grid independence test

Element size (mm)	Number of elements	Nodes	Base Temperature (K)
18	1155656	227043	299.86548
15	1174251	230811	299.92877
12	1225566	240647	299.78117
9	1377670	270093	299.83811
6	2514225	483138	299.83290

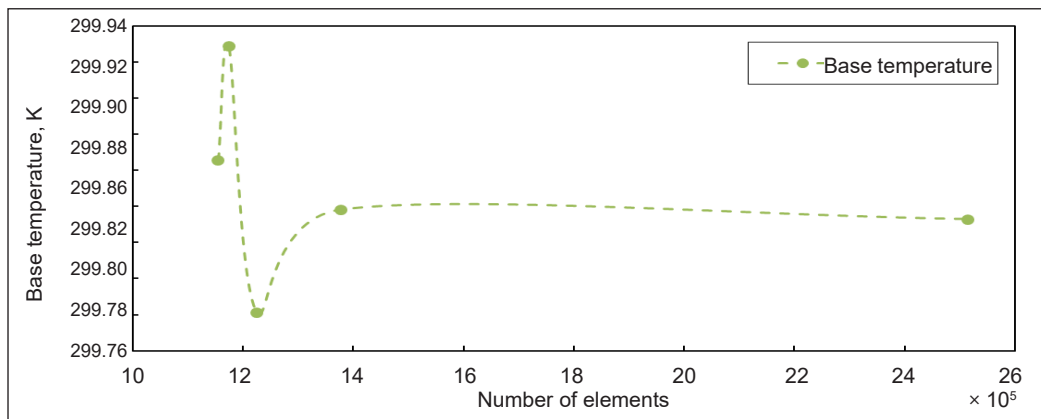


Figure 5. Mesh sensitivity analysis of grid independence test

Governing Equations

Natural convection flows have been simulated under the assumption of laminar, steady and incompressible flow conditions and the Boussinesq approximation. The governing equations related to this study are shown in Equations 2–7 (Effendi et al., 2018; Hoffmann & Chiang, 2000).

Based on the mass conservation principle, the following continuity Equation 2 can be expressed below:

$$\frac{\partial u}{\partial x} + \frac{\partial v}{\partial y} + \frac{\partial w}{\partial z} = 0 \tag{2}$$

Under heating conditions, the natural convection flow is driven by the air density change and gravity force. Therefore, for natural convection flow, the momentum Equations 3–5 can be written can be expressed as below:

$$u \frac{\partial u}{\partial x} + v \frac{\partial u}{\partial y} + w \frac{\partial u}{\partial z} = -\frac{1}{\rho} \frac{\partial P}{\partial x} + \nu \left(\frac{\partial^2 u}{\partial x^2} + \frac{\partial^2 u}{\partial y^2} + \frac{\partial^2 u}{\partial z^2} \right) \quad [3]$$

$$u \frac{\partial v}{\partial x} + v \frac{\partial v}{\partial y} + w \frac{\partial v}{\partial z} = -\frac{1}{\rho} \frac{\partial P}{\partial y} + \nu \left(\frac{\partial^2 v}{\partial x^2} + \frac{\partial^2 v}{\partial y^2} + \frac{\partial^2 v}{\partial z^2} \right) \quad [4]$$

$$u \frac{\partial w}{\partial x} + v \frac{\partial w}{\partial y} + w \frac{\partial w}{\partial z} = -\frac{1}{\rho} \frac{\partial P}{\partial z} + \nu \left(\frac{\partial^2 w}{\partial x^2} + \frac{\partial^2 w}{\partial y^2} + \frac{\partial^2 w}{\partial z^2} \right) + g\beta(T - T_\infty) \quad [5]$$

The energy equation is obtained based on energy balance characteristics. For example, the energy Equation 6 for the fluid region is expressed as below:

$$u \frac{\partial T}{\partial x} + v \frac{\partial T}{\partial y} + w \frac{\partial T}{\partial z} = \alpha \left(\frac{\partial^2 T}{\partial x^2} + \frac{\partial^2 T}{\partial y^2} + \frac{\partial^2 T}{\partial z^2} \right) \quad [6]$$

The energy equation for the solid region is expressed as Equation 7:

$$\left(\frac{\partial^2 T}{\partial x^2} + \frac{\partial^2 T}{\partial y^2} + \frac{\partial^2 T}{\partial z^2} \right) = 0 \quad [7]$$

Where u, v and w are the velocities in the direction of x, y and z , respectively. While P is pressure, ρ is density, g is the gravitational acceleration constant, β is volumetric expansivity, ν is kinematic viscosity, T is temperature, T_∞ is free stream temperature, and α is thermal diffusivity.

RESULTS AND DISCUSSION

Validation of Simulation with Experimental data from Literature

In order to justify the accuracy of the simulation of this research, the validation was done by quoting the experimental results from literature (Effendi & Kim, 2015). Therefore, this study did run a simulation base on operating parameters from literature (Effendi & Kim, 2015). The simulation was then compared with the experimental results from the literature (Effendi & Kim, 2015). The validation of the results in this study with the previous study is related to the effect of fins spacing on thermal resistance. Thermal resistance is one of the most important parameters for determining heat sinks' heat transfer characteristics and designing an electronic cooling device. In this study, the same geometrical configuration

of the experimental models was adopted for the simulation models for validation. The same fins spacing was adopted for the simulation and tested with a heat source of 5W and 30W. The comparison of results for validation was considered for both Solid Hybrid Fin heat sink (SHF HS) and Pin Fins heat sink (PF HS) since only that designs correlate with the designs in this study. It is to ensure the results are comparable and can be validated. Thermal resistance was the main parameter for testing the validity of the simulation with experimental work. Thermal resistance, R_{th} can be expressed as Equation 8:

$$R_{th} = \frac{T_b - T_a}{q} \tag{8}$$

Where T_b is the temperature of the base of heat sink, T_a is ambient air temperature and q is rate of heat transfer (Effendi & Kim, 2018). Table 4 shows the results for thermal resistance against different fins spacing.

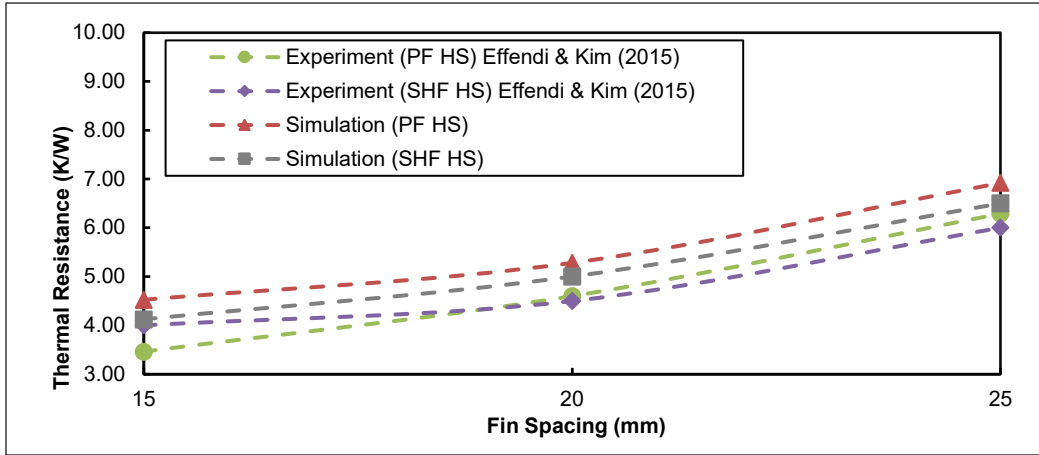
Table 4
Results of thermal resistance for both simulation and experimental from Effendi & Kim (2015)

Power (W)	Fin spacing (mm)	Thermal resistance (K/W) (Experimental)		Thermal resistance (K/W) (Simulation)	
		Solid Hybrid Fins Heat Sink	Pin Fins Heat Sink	Solid Hybrid Fins Heat Sink	Pin Fins Heat Sink
5	15	4.00	3.46	4.12	4.52
	20	4.50	4.60	5.00	5.28
	25	6.00	6.29	6.50	6.92
30	15	2.27	2.67	2.99	3.00
	20	3.00	3.49	4.30	4.00
	25	4.00	4.57	5.30	5.00

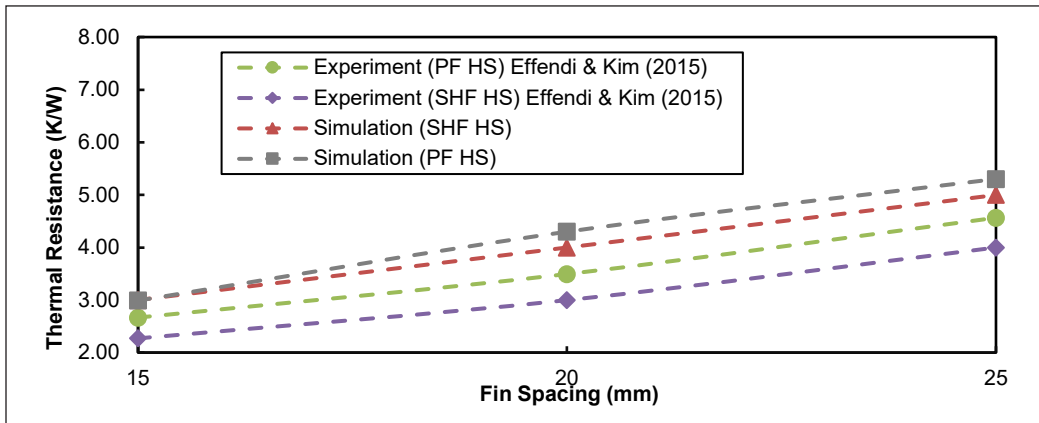
Table 5
MAPE Error percentages between simulation and experimental results

Power (W)	Average of MAPE Error percentage (%) (SHF HS)	Average of MAPE Error percentage (%) (PF HS)
5	11.40	10.11
30	10.34	10.56

Figure 6 is quite revealing in several ways. First, as indicated in Figures 6(a) and 6(b), the predicted thermal resistance is slightly higher than the experimental results. The reason is that, whereas the pins are in perfect contact with the upper bottom plate in the simulation, it is not so in the experiment. The limiting factor of the viscous laminar model could also contribute to the difference, as reported in (Lu & Jiang, 2006). The relationship between thermal resistance and fin spacing is directly proportional, and the results from



(a)



(b)

Figure 6. Validation of results of Thermal Resistance of HPFWC HS and PFWC HS against Fin Spacing on heat at (a) 5W and (b) 30W

simulations produce a similar result to the previous study by Effendi and Kim (2015). The second reason for the disparity between the simulation and experiment is that the aluminium used for the experiment is Aluminium 6063, which has slightly different properties than standard aluminium used in simulations. To further prove the validity of the simulation, the error between the simulations results and the previous study was calculated using the Mean Absolute Percentage Error (MAPE) formula. The formulation of MAPE can be expressed as Equation 9:

$$MAPE = \frac{100}{N} \times \sum_{i=1}^N \left| \frac{x_i - \hat{x}_i}{x_i} \right| \quad [9]$$

N , x_i and \hat{x}_i is the representatives of the number of values, simulation and experimental values, respectively. From the analysis using Equation 9, all validation errors are about 10%,

which can be referred to in Table 5. Based on these percentage errors that are relatively less than 12%, it can be concluded that the present model is significantly accurate to predict the thermal resistance of the heat sink.

Thermal and Flow Fields

Figures 7 and 8 show airflow’s temperature distributions and velocity profile around each heat sink. Figure 7 shows the temperature distributions between the two designs. It can be observed that the edges of PFWC HS are at a lower temperature than the central region. In comparison, the temperature distributions in HPFWC HS show an irregular pattern, with some of the pin fins at lower temperatures than others. The central region does not show any significant difference from the edges.

Table 6 shows the result of the base temperature for each heat sink. At the same heat flux, the base temperature of HPFWC HS Type 1 is higher compared to PFWC HS Type 1. The reason is that the surface area of HPFWC HS is higher than that of PFWC HS, and the wings around the HPFWC HS promote swirl flows and fluid mixing; this situation interrupts the thermal boundary layer through the HPFWC HS. It leads to a higher heat transfer coefficient, higher heat dissipation and higher baseplate temperature. This result is consistent with the result found in Acharya and Dash (2018).

Figures 8(a) to 8(d) show the velocity profile of the airflow around each heat sink. Although the flow pattern of air around each heat sink shows a non-uniform flow, it can be observed that some regions of high-velocity profile result in high vortex formation. For example, a comparison of airflow profile between HPFWC HS and PFWC HS shows a high-velocity profile of air around HPFWC HS than PFWC HS, resulting in high vortex formation around HPFWC HS than PFWC HS. The reason is that the wings around the HPFWC HS cause an irregular flow pattern of the air which eventually induces high vortex formation.

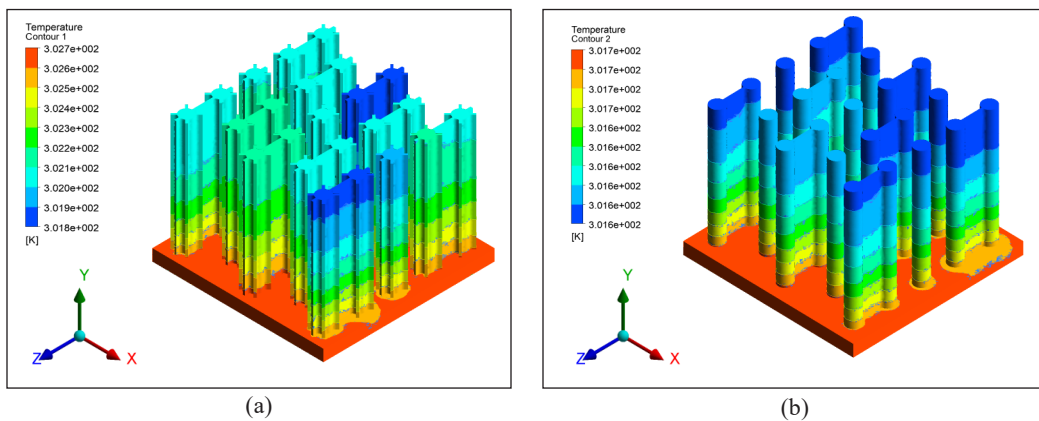


Figure 7. Temperature distributions (a) HPFWC HS (b) PFWC HS

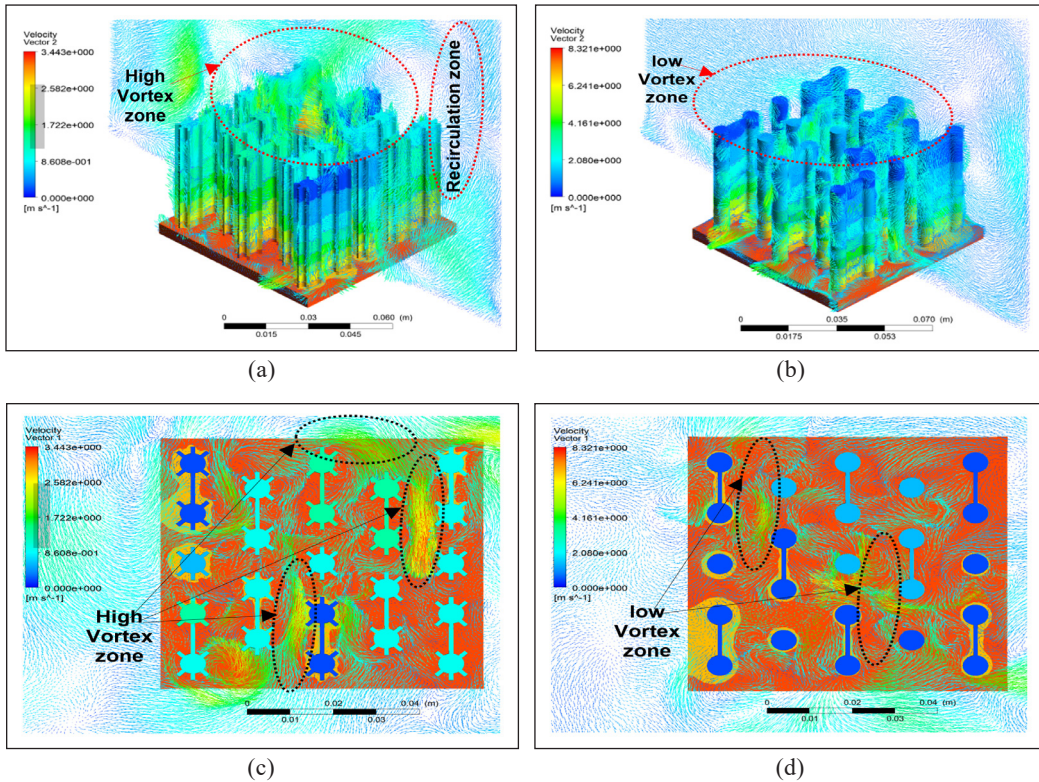


Figure 8. Airflow velocity profile around (a) Isometric view of HPFWC HS (b) Isometric view of PFWC HS (c) Top view of HPFWC HS (d) Top view of PFWC HS

Thermal Performances

Generally, the performance of a heat sink is a measure of the temperature difference between the bottom plate and atmospheric air ΔT . The ΔT is, however, a function of the rate of heat applied Q . Temperature differences can be expressed as Equation 10

$$\Delta T = T_b - T_a \quad [10]$$

Where T_b is the temperature of base of heat sink and T_a is ambient air temperature.

Figure 9 shows a linear variation in ΔT with respect to the heat applied to the base plate. Interestingly, both designs' heat sink type 3 shows a higher temperature difference. The reason is that heat sink type 3 has lower fin spacing. Thus, the heat dissipation rate from local hot spots on the plate to the fins is much higher, promoting higher fluid interaction with the solid surface and enhancing convective heat transfer. On the other hand, heat sink type 1 has a lower temperature difference because the higher fin spacing associated with heat sink type 1 does not enhance heat dissipation from hot spots on the base plate. Hence, heat sinks type 1 has a lower base temperature.

From the results in Figure 9, other parameters can also be calculated. As mentioned earlier, the following parameters for HPFWC HS Type 1 and PFWC HS Type 1 can be found in Table 6. All calculations are done by using Ansys FLUENT. The parameters that have been calculated are thermal conductivity, k , Prandlt number, Pr , Grashof number, Gr and Rayleigh number, Ra .

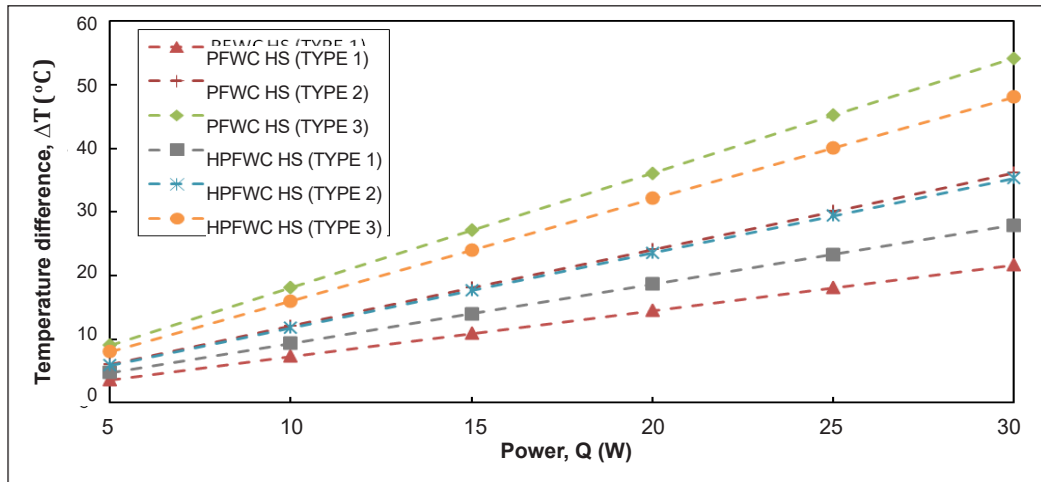


Figure 9. Graph of temperature differences, ΔT against the power input, Q tested for all configurations of heat sinks.

Table 6
Thermal parameters of HPFWC HS Type 1 and PFWC HS Type 1

Heat Sink	Power (W)	Base Temperature (°C)	T_{film} (°C)	k (W/m.K)	Pr	Gr	Ra
PFWC Type 1	5	28.6	26.8	0.02564	0.7291	4.725×10^2	3.445×10^2
	10	32.3	28.7	0.02578	0.7286	9.320×10^2	6.791×10^2
	15	35.9	30.5	0.02592	0.7281	1.354×10^3	9.861×10^2
	20	39.5	32.3	0.02605	0.7276	1.754×10^3	1.276×10^3
	25	43.1	34.1	0.02618	0.7271	2.132×10^3	1.550×10^3
	30	46.7	35.9	0.02632	0.7266	2.492×10^3	1.811×10^3
HPFWC Type 1	5	29.7	27.4	0.02569	0.7289	6.118×10^2	4.460×10^2
	10	34.3	29.7	0.02586	0.7283	1.170×10^3	8.523×10^2
	15	39.0	32.0	0.02603	0.7276	1.701×10^3	1.238×10^3
	20	43.6	34.3	0.02620	0.7270	2.186×10^3	1.589×10^3
	25	48.3	36.7	0.02638	0.7264	2.644×10^3	1.920×10^3
	30	52.9	39.0	0.02655	0.7258	3.061×10^3	2.222×10^3

The relationship between base temperature, T_b and other parameters has been observed. The first parameter observed is a relation between base temperature, T_b and thermal conductivity, k . The thermal conductivity data was a result of simulation from

CFD Ansys. It can be observed from Figure 10 that there is a linear correlation between thermal conductivity and base temperature. Interestingly both HPFWC HS and PFWC HS showed similar characteristics in responding to changes in thermal conductivity. This phenomenon is because, as expected, any increase in the thermal conductivity is always accompanied by an increase in heat transfer characteristics of that material.

Prandtl number, Pr has also been calculated to observe its relationship with base temperature, T_b . Then, the Prandtl number, Pr , can be expressed as Equation 11:

$$Pr = \frac{\nu}{\alpha} \quad [11]$$

Where ν is the momentum diffusivity and α is the thermal diffusivity. Figure 11 shown that as T_b increases, Pr is decreases for both heat sinks. HPFWC HS has lower Pr than PFWC HS which is 8.72% lower. Since the heat transfer rate is better in lower Pr , HPFWC HS has performed better efficiently dissipating heat into the ambient.

Table 7 shows the tabulated data of thermal performances of HPFWC HS Type 1 and PFWC HS Type 1.

Table 7
Thermal performances of HPFWC HS Type 1 and PFWC HS Type 1

Heat Sink	Base Temperature (°C)	Nu	h (W/m ² .K)
PFWC Type 1	28.6	2.96	5.062
	32.3	3.50	6.023
	35.9	3.85	6.645
	39.5	4.10	7.121
	43.1	4.30	7.512
	46.7	4.47	7.851
HPFWC Type 1	29.7	3.16	5.407
	34.3	3.71	6.393
	39.0	4.07	7.061
	43.6	4.33	7.565
	48.3	4.54	7.984
	52.9	4.71	8.333

$$h = \frac{Q}{A_s \Delta T} \quad [12]$$

The heat transfer coefficient, h , can be expressed as Equation 12 (Meng et al., 2018): Where Q is the input power, A_s is heat sink surface area, and ΔT is the temperature difference. While Nu that been used in this study is expressed by Shen et al. (2016) as Equation 13:

$$Nu = \frac{1}{0.25(((\pi(D + H)/N) - t)Ra^{0.13}/L)^{-1.7} + 1} \times \left(0.68 + \frac{0.670Ra^{1/4}}{\left(1 + (0.492/Pr)^{9/16}\right)^{4/9}} \right) \quad [13]$$

Which is also equivalent to Equation 14:

$$Nu = \frac{hL_c}{k} \quad [14]$$

Where h is convective heat transfer coefficient, L_c is characteristics length, and k is thermal conductivity. The hydraulic length for the heat sink is the fin spacing, S which depends on the respective spacing (Effendi et al., 2018). Rayleigh Number, Ra is a product of Grashof Number, Gr and Prandlt Number, Pr , which can be expressed as Equation 15:

$$Ra = Gr.Pr \quad [15]$$

Which Gr can be expressed as Equation 16

$$Gr = \frac{g\beta(T_b - T_\infty)L_c^3}{\nu^2} \quad [16]$$

Where g is gravity, β is thermal coefficient expansion, T_b is base temperature, T_∞ is free stream temperature, L_c characteristics length and ν is kinematic viscosity.

Figure 12 shows that as Ra increases, Nu also increases. HPFWC HS has the highest Nu while PFWC HS has the lowest Nu . The difference between the highest Nu of HPFWC HS and PFWC HS is 5.78%. From Figure 13, both heat sinks show some similarity, but the highest h results from HPFWC HS. It is proven again that HPFWC HS has better performance in heat transfer than PFWC HS.

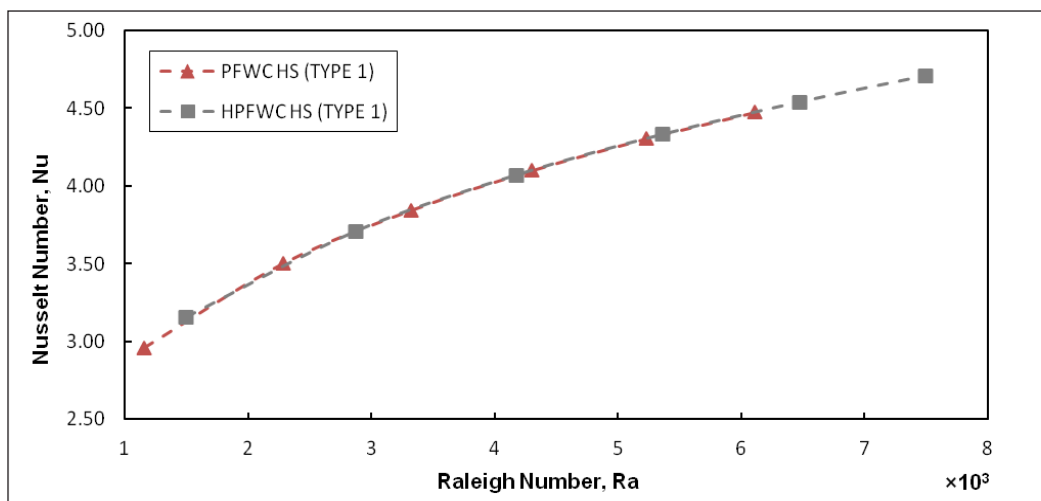


Figure 12. The relation of Nusselt number, Nu and Rayleigh number, Ra

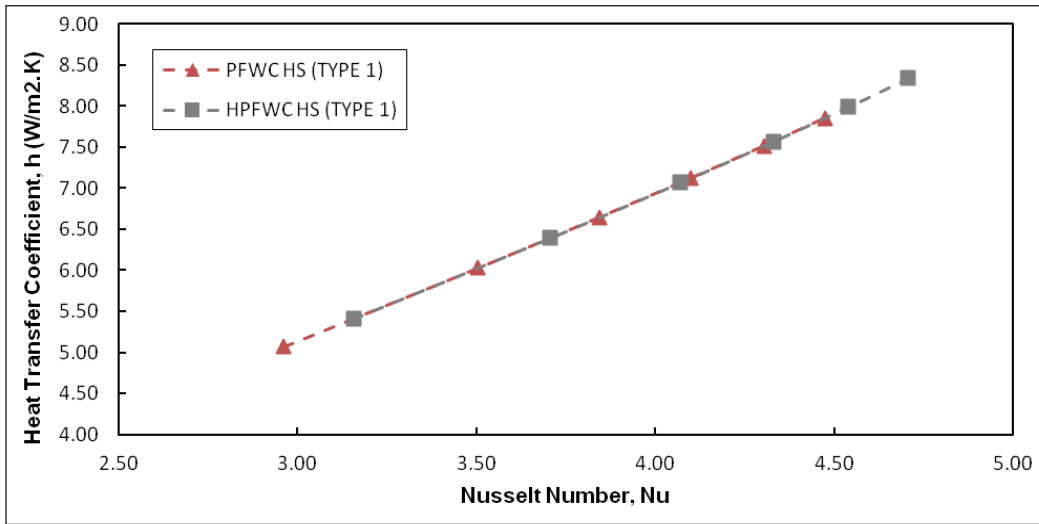


Figure 13. The relation of heat transfer coefficient, h and Nusselt number, Nu

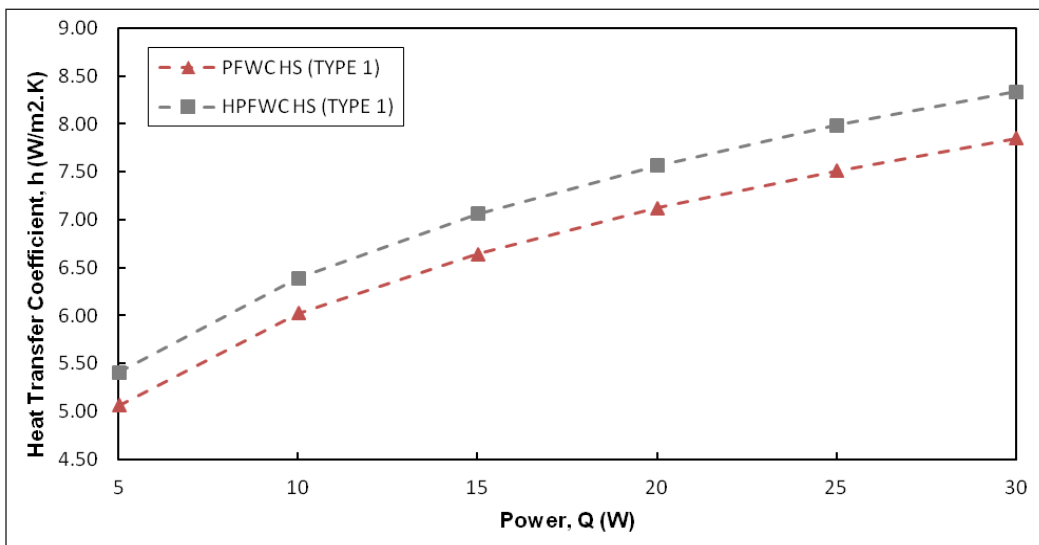


Figure 14. The relation of heat transfer coefficient, h and input power, Q

This study obtained the heat transfer coefficient, h , using Equation 14 with the Nu equation in Equation 13. The relationship between h and Nu is illustrated in Figure 13, and the effect of power input Q at the base of the heat sink is shown in Figure 14. The variation of input power, Q , has also been observed to increase slowly for h . Interestingly, HPFWC HS Type 1 shows a higher value of h for any variation of Q . The reason is that the wings attached to the pin fins of HPFWC HS Type 1 generate swirl flow which enhances the mixing of the fluid and interrupts the thermal boundary layer; this effect contributes to

an increase in h . This finding is consistent with Hosseinirad et al. (2019). Furthermore, the average difference between h of HPFWC HS and PFWC HS is 5.94%. Therefore, HPFWC HS Type 1 dissipates heat at 5.94% more than PFWC HS.

Fin Spacing Effect

Figure 15 shows the effect of fin spacing on the heat transfer coefficient of the heat sink under consideration. As can be observed, there is a linear increase in heat transfer coefficient with an increase in fin spacing. A possible explanation for these results may be that increasing pin fin spacing promotes more influx of fluid, enhances the interaction between the fluid flow across the solid surface. There was a significant difference between the two heat sinks. For example, at a fin spacing of 20mm, the heat transfer coefficient for HPFWC HS Type 1 is higher than that of PFWC HS type 1 by about 5%. The reason is that the heat sink HPFWC HS Type 1 has wings around it, and these wings help to promote vortex formation around the fins, and it is this vortex formation that enhances the heat transfer characteristics. This finding is similar to that of Haghghi et al. (2018).

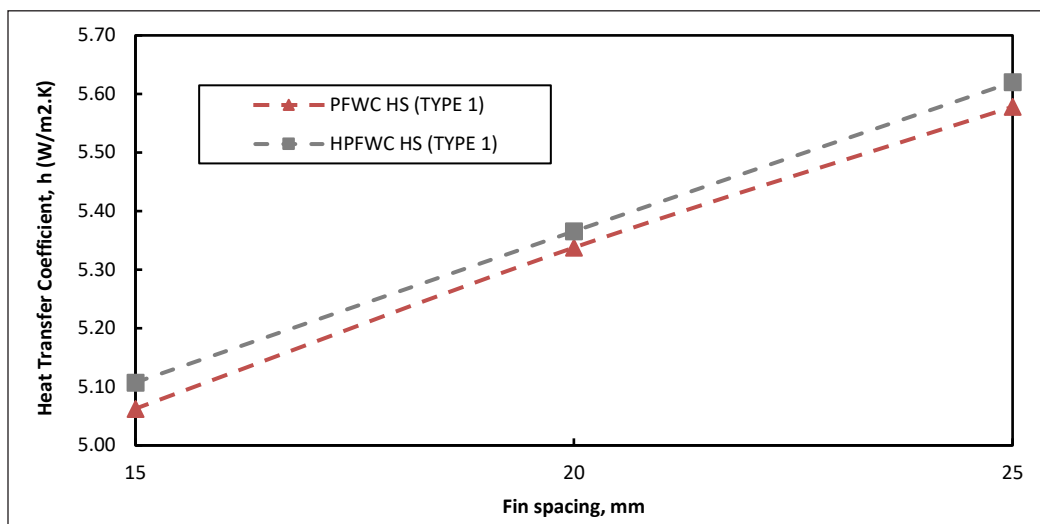


Figure 15. Fin spacing, S effect on heat transfer coefficient, h

CONCLUSION AND RECOMMENDATIONS

This study has numerically determined the thermal performances of Hybrid Pin Fin with Connector (HPFWC HS) and Pin Fin Heat Sink (PFWC HS). Three configurations were analysed based on the different spacing of the fins. The simulation was done to numerically determine the thermal parameters of the heat sinks under natural convection conditions and thermal performances. The simulation was validated with previous studies to observe

the correlation and the performances between designs of heat sinks. In this study, the results for validating the Ansys CFD simulation with experiment show about 12% error. It indicates how close was the simulation result with the experiment. Interestingly both HPFWC HS and PFWC HS showed similar characteristics in responding to changes in thermal conductivity. The reason for this output is that increasing thermal conductivity is always accompanied by increasing heat transfer characteristics. Also, increasing pin fin spacing promotes more influx of fluid, enhancing interaction between the fluid flow across the solid surface. However, there was a significant difference between the two heat sinks. For example, at a fin spacing of 20mm, the heat transfer coefficient for HPFWC HS Type 1 is higher than that of PFWC HS type 1 by about 5%. In conclusion, increasing the number of fins increases the total area and increases the heat transfer rate.

ACKNOWLEDGEMENT

The authors want to express their appreciation to the Universiti Teknologi MARA (UiTM) through the Geran Penyelidikan Khas UiTM (Grant No. 600-RMC/GPK 5/3 (133/2020)) for funding this research.

REFERENCES

- Acharya, S., & Dash, S. K. (2018). Natural convection heat transfer from a horizontal hollow cylinder with internal longitudinal fins. *International Journal of Thermal Sciences*, 134, 40-53. <https://doi.org/10.1016/j.ijthermalsci.2018.07.039>
- Arefin, A. M. E. (2016). Thermal analysis of modified pin fin heat sink for natural convection. In *2016 5th International Conference on Informatics, Electronics and Vision, ICIEV 2016* (pp. 1-5). IEEE Publishing. <https://doi.org/10.1109/ICIEV.2016.7759986>
- Choudhary, V., Kumar, M., & Patil, A. K. (2019). Experimental investigation of enhanced performance of pin fin heat sink with wings. *Applied Thermal Engineering*, 155, 546-562. <https://doi.org/10.1016/j.applthermaleng.2019.03.139>
- Effendi, N. S., & Kim, K. J. (2015). Thermal behaviours of passively-cooled hybrid fin heat sinks for lightweight and high performance thermal management. In *Proceedings of the ASME 2015 International Technical Conference and Exhibition on Packaging and Integration of Electronic and Photonic Microsystems InterPACK2015* (pp. 1-7). American Society of Mechanical Engineers.
- Effendi, N. S., & Kim, K. J. (2018). Natural convective hybrid fin heat sinks for lightweight and high performance thermal management. *Journal of Mechanical Science and Technology*, 32(10), 5005-5013. <https://doi.org/10.1007/s12206-018-0948-4>
- Effendi, N. S., Putra, S. S. G. R., & Kim, K. J. (2018). Prediction methods for natural convection around hollow hybrid fin heat sinks. *International Journal of Thermal Sciences*, 126, 272-280. <https://doi.org/10.1016/j.ijthermalsci.2018.01.002>

- Haghighi, S. S., Goshayeshi, H. R., & Safaei, M. R. (2018). Natural convection heat transfer enhancement in new designs of plate-fin based heat sinks. *International Journal of Heat and Mass Transfer*, *125*, 640-647. <https://doi.org/10.1016/j.ijheatmasstransfer.2018.04.122>
- Hoffmann, K. A., & Chiang, S. T. (2000). *Computational fluid dynamics* (Vol. 1). Engineering Education System.
- Hosseini-rad, E., Khoshvaght-Aliabadi, M., & Hormozi, F. (2019). Effects of splitter shape on thermal-hydraulic characteristics of plate-pin-fin heat sink (PPFHS). *International Journal of Heat and Mass Transfer*, *143*, Article 118586. <https://doi.org/10.1016/j.ijheatmasstransfer.2019.118586>
- Humphries, J. (2014). *Thermal management of electronics devices - The role it plays*. Electrolube. https://electrolube.com/knowledge_base/thermal-management-of-electronics-devices/
- Ibrahim, T. K., Mohammed, M. N., Mohammed, M. K., Najafi, G., Sidik, N. A. C., Basrawi, F., Abdalla, A. N., & Hoseini, S. S. (2018). Experimental study on the effect of perforations shapes on vertical heated fins performance under forced convection heat transfer. *International Journal of Heat and Mass Transfer*, *118*, 832-846. <https://doi.org/10.1016/j.ijheatmasstransfer.2017.11.047>
- Immerman, G. (2017). *Why industry 4.0 is important and why manufacturers should care*. Machinemetrics. <https://www.machinemetrics.com/blog/why-industry-4-0-is-important>
- Jassem, R. R. (2013). Effect the form of perforation on the heat transfer in the perforated fins. *Academic Research International*, *4*(3), 198-207. <https://doi.org/10.13140/RG.2.1.2437.0326>
- Jensen, M. (2018). *The importance of proper meshing in finite element analysis*. Steen Solutions. <http://steensolutions.com/2017/01/importance-proper-meshing-finite-element-analysis/>
- Joo, Y., & Kim, S. J. (2015). Comparison of thermal performance between plate-fin and pin-fin heat sinks in natural convection. *International Journal of Heat and Mass Transfer*, *83*, 345-356. <https://doi.org/10.1016/j.ijheatmasstransfer.2014.12.023>
- Kumar, V. M., Farooq, S., & Rao, B. N. (2016). A detailed review on pin fin heat sink. *International Journal of Energy and Power Engineering*, *10*(5), 1006-1015.
- Lu, B., & Jiang, P. X. (2006). Experimental and numerical investigation of convection heat transfer in a rectangular channel with angled ribs. *Experimental Thermal and Fluid Science*, *30*(6), 513-521. <https://doi.org/10.1016/j.exptthermflusci.2005.09.007>
- Meng, X., Zhu, J., Wei, X., & Yan, Y. (2018). Natural convection heat transfer of a straight-fin heat sink. *International Journal of Heat and Mass Transfer*, *123*, 561-568. <https://doi.org/10.1016/j.ijheatmasstransfer.2018.03.002>
- Nada, S. A., & Said, M. A. (2019). Effects of fins geometries, arrangements, dimensions and numbers on natural convection heat transfer characteristics in finned-horizontal annulus. *International Journal of Thermal Sciences*, *137*, 121-137. <https://doi.org/10.1016/j.ijthermalsci.2018.11.026>
- Perry, J. (2017). *Thermal comparison of copper and aluminum heat sinks*. Advanced Thermal Solutions Inc. <https://www.qats.com/cms/2017/03/28/case-study-thermal-comparison-copper-aluminum-heat-sinks/>
- Schelling, P. K., Shi, L., & Goodson, K. E. (2005). Managing heat for electronics. *Materials Today*, *8*(6), 30-35. [https://doi.org/10.1016/S1369-7021\(05\)70935-4](https://doi.org/10.1016/S1369-7021(05)70935-4)

- Shen, Q., Sun, D., Xu, Y., Jin, T., Zhao, X., Zhang, N., Wu, K., & Huang, Z. (2016). Natural convection heat transfer along vertical cylinder heat sinks with longitudinal fins. *International Journal of Thermal Sciences*, 100, 457-464. <https://doi.org/10.1016/j.ijthermalsci.2015.09.007>
- Vijay, V. (2019). *Free and forced convection study notes for mechanical engineering*. Gradeup. <https://gradeup.co/free-and-forced-convection-i-9d6951ec-c265-11e5-9f7c-7aa8072720c6>
- Zagala, E. J. (2016). Heat conductivity. In B. Bhushan (Ed.), *Encyclopedia of Nanotechnology* (pp. 1453-1453). Springer. https://doi.org/10.1007/978-94-017-9780-1_100385
- Zaidshah, S., & Yadav, V. (2019). Heat transfer from different types of fins with notches with varying materials to enhance rate of heat transfer: A review. *International Journal of Applied Engineering Research*, 14(9), 174-179.